Available online at www.sciencedirect.com
SCIENCE DIRECT®

Journal of Catalysis 235 (2005) 229–240

JOURNAL OF CATALYSIS

www.elsevier.com/locate/jcat

Intermediates in the hydrodesulfurization of 4,6-dimethyl-dibenzothiophene over Pd/γ-Al_2O_3

Adeline Röthlisberger, Roel Prins [*]

Institute for Chemical and Bioengineering, Swiss Federal Institute of Technology (ETH), 8093 Zurich, Switzerland

Received 3 June 2005; revised 5 August 2005; accepted 7 August 2005

Abstract

The hydrodesulfurization (HDS) reaction network of 4,6-dimethyl-dibenzothiophene (4,6-DM-DBT) was investigated over Pd/γ-Al_2O_3 at 300 °C and 5 MPa. 4,6-DM-DBT reacts almost exclusively through the hydrogenation pathway, with only 1% reacting via the direct desulfurization route. No significant further hydrogenation of the desulfurized compounds occurred. Three (partially) hydrogenated intermediates of the HYD pathway were observed: 4,6-dimethyl-1,2,3,4-tetrahydro-dibenzothiophene (4,6-DM-TH-DBT), 4,6-dimethyl-hexahydro-dibenzothiophene (4,6-DM-HH-DBT), and 4,6-dimethyl-perhydro-dibenzothiophene (4,6-DM-PH-DBT). These three intermediates were synthesized and their HDS studied. Hydrogenation and dehydrogenation reactions occurred readily between the intermediates. 4,6-DM-TH-DBT and 4,6-DM-HH-DBT interconverted rapidly and were in equilibrium in the HDS of 4,6-DM-DBT and close to equilibrium in the experiments starting from the intermediates. The partly saturated 4,6-DM-TH-DBT and 4,6-DM-HH-DBT intermediates could be desulfurized much easier than 4,6-DM-DBT. This shows that the molecule planarity must be removed to weaken the steric hindrance caused by the methyl groups and to provide better access to the sulfur atom. Temperature had a stronger promotional effect on desulfurization than on hydrogenation and enhanced sulfur removal from the reaction intermediates.

Keywords: Hydrodesulfurization; 4,6-Dimethyl-dibenzothiophene; Partially hydrogenated intermediates; Mechanism; Palladium; Hydrogenation

1. Introduction

The maximum allowed amount of sulfur in gasoline and diesel fuel was reduced to 50 ppm in many parts of the world in 2005 and probably will be reduced even further by the end of the decade. Deep hydrodesulfurization (HDS) technology must be implemented to attain this low level of sulfur. Molecules such as 4,6-dialkyl-dibenzothiophene, with alkyl groups adjacent to the sulfur atom, are very difficult to desulfurize and are problematic in deep HDS [1,2]. 4,6-Dimethyl-dibenzothiophene (4,6-DM-DBT) is therefore commonly used as a model molecule in HDS studies.

Extensive research with metal sulfide catalysts has shown that the HDS of dibenzothiophene (DBT) and 4,6-DM-DBT occurs by two reaction pathways [1–3]. In the direct desulfurization (DDS) pathway, the C–S bonds of the reactant molecule are broken by hydrogenolysis, leading to the formation of 3,3′-dimethyl-biphenyl. In the hydrogenation (HYD) pathway, the reactant molecule is first hydrogenated to intermediates, the C–S bonds of which are then broken to form 3,3′-dimethyl-cyclohexylbenzene and 3,3′-dimethyl-bicyclohexyl. Whereas the HDS of DBT occurs mainly by the DDS pathway, the HYD pathway dominates the HDS of 4,6-DM-DBT. A generally accepted explanation for this phenomenon is that in the DDS pathway, the reactant must adsorb in a σ mode, perpendicular to the catalyst surface. In this mode, the neighboring methyl groups hinder bonding with the catalytic sites because they extend further into space than the lone pairs of the sulfur atom, which are responsible for the σ bonding.

The HDS of 4,6-DM-DBT is dominated by the HYD pathway and thus depends on the hydrogenating ability of the catalyst. Because metals are much better hydrogenation catalysts than metal sulfides, metal catalysts might be suitable for deep HDS. Unfortunately, metal catalysts are thermodynamically un-

---

[*] Corresponding author.
E-mail addresses: jcat@tech.chem.ethz.ch, roel.prins@chem.ethz.ch (R. Prins).

0021-9517/$ – see front matter © 2005 Elsevier Inc. All rights reserved.
doi:10.1016/j.jcat.2005.08.007

stable in the presence of sulfur-containing molecules, and the metal particles may change in metal sulfide particles. The noble metals on the right side of the periodic table should be less sensitive to sulfur; indeed, several investigations have shown that Pt and Pd in particular are less susceptible to transformation to inactive sulfides than other metals. Furthermore, the support has been shown to play an important role, with such supports as zeolites and silica–alumina stabilizing Pt particles much better than other supports. Thus the influence of the metal and the support on the hydrogenation of aromatics in diesel fuel over PtPd on amorphous silica–alumina (ASA) [4], benzene over Pt/zeolite MOR and Pt/LTL [5–7], toluene [8] and tetralin [9] over PtPd/Al_2O_3, toluene and naphthalene over PtPd/ASA [10], toluene over PtPd/ASA and PtPd/zeolite Y [11], naphthalene over PtPd/Mg–Al oxide [12], and tetralin over PtPd/ZrO_2-MCM [13] have been studied.

Few studies on the HDS properties of noble metals have been published, however, and these dealt only with their general activities and the DDS to HYD ratios [14–19]. Therefore, we started with an investigation of the reaction network of the HDS of 4,6-DM-DBT over Pd, because this metal has been reported to have the best resistance against H_2S. Because this network is complex, it is not enough to study only the reaction of 4,6-DM-DBT; the reactions of some or all of the intermediates should be studied as well. Therefore, we synthesized three key intermediates—4,6-dimethyl-1,2,3,4-tetrahydro-dibenzothiophene (4,6-DM-TH-DBT), 4,6-dimethyl-1,2,3,4,4a,9b-hexahydro-dibenzothiophene (4,6-DM-HH-DBT), and 4,6-dimethyl-perhydro-dibenzothiophene (4,6-DM-PH-DBT)—and studied their HDS in addition to that of 4,6-DM-DBT. We addressed the following questions: How does the DDS occur, and how does the last part of the HYD—that is, the final removal of sulfur from the hydrogenated DBT intermediates—occur?

2. Experimental

2.1. HDS experiments

All of the experiments were performed over a 0.50 wt% Pd on γ-Al_2O_3 catalyst (Condea, 35–60 mesh ≈ 400–250 µm, BET surface area 220 m^2/g, total pore volume 0.6 ml/g, metal dispersion 56% as calculated from the strong hydrogen chemisorption), diluted with SiC in a continuous mode in a fixed-bed Inconel reactor [20]. We used 50 mg of catalyst in the HDS experiments with 4,6-DM-DBT and 20 mg of catalyst for the more reactive hydrogenated intermediates. Before the HDS experiments, the catalyst was activated by in situ reduction in a 50 nml/min hydrogen flow at 300 °C and 0.5 MPa for 2 h. Then the total pressure was increased to the reaction pressure of 5 MPa, and the liquid reactants were fed to the reactor. Most of the HDS and hydrogenation experiments were performed at 300 °C; only one HDS experiment with 4,6-DM-DBT was done at 280 °C. The gas phase feed consisted of 130 kPa decane (as solvent), 8 kPa dodecane (as internal standard), 1 kPa sulfur-containing reactant, and ∼4.85 MPa hydrogen. The following sulfur-containing reactants were used: 4,6-DM-DBT (Acros; 95%) and its partially and fully hydrogenated derivatives 4,6-DM-TH-DBT, 4,6-DM-HH-DBT, and 4,6-DM-PH-DBT. These sulfur-containing intermediates were prepared in our laboratory by (partial) hydrogenation of 4,6-DM-DBT, as described herein. Possible further hydrogenation of the desulfurized reaction products was investigated through a hydrogenation experiment with 1 kPa 3,3′-dimethyl-biphenyl (3,3′-DM-BP, 99%; Aldrich). To simulate the presence of sulfur components in the system, the reaction was done in the presence of 1 kPa dibenzothiophene (DBT, 98%; Fluka). To diminish a possible influence of catalyst deactivation, all investigations of the conversion and product yields as a function of weight time started at the highest weight time (lowest flow rate), with the weight time decreased thereafter. We expected palladium to be partly sulfided under these experimental conditions [21].

2.2. Preparation of 4,6-DM-TH-DBT

The production of 4,6-DM-TH-DBT was performed in a similar reactor as used in the HDS experiments. The reactor was loaded with 400 mg 8 wt% Mo/γ-Al_2O_3 prepared by incipient wetness impregnation [22]. Before the reaction, the catalyst was activated by in situ sulfidation with a mixture of 10% H_2S in H_2 (50 nml/min) at 400 °C and 1 MPa for 4 h. The temperature was decreased to 320 °C, and the total pressure was increased to 5 MPa, and then the liquid reactants were fed to the reactor. The gas phase feed consisted of 130 kPa toluene (as solvent), 2.5 kPa 4,6-DM-DBT (almost the limit of solubility, 45 mg/ml), 20 kPa H_2S, and ∼4.85 MPa H_2. The reaction was carried out at weight time $\tau = 4.9\ \mathrm{g\,min/mol}$. Under these conditions, the product mixture consisted of 69% 4,6-DM-DBT, 18% 4,6-DM-TH-DBT, 6.5% 4,6-DM-HH-DBT, 0.5% 4,6-DM-PH-DBT, and 6% desulfurized products.

After partial evaporation of the solvent, unreacted 4,6-DM-DBT was recovered by crystallization in toluene and separation by filtration. The remaining mother liquor was added to commercial silica and evaporated to dryness. The reaction products were separated by column chromatography over silica, using petrol ether as the eluent. The fractions containing 4,6-DM-TH-DBT were further purified by vacuum distillation. MS, ^1H, and ^{13}C NMR spectroscopy revealed the final product to be 4,6-dimethyl-1,2,3,4-tetrahydro-dibenzothiophene.

2.3. Preparation of 4,6-DM-HH-DBT and 4,6-DM-PH-DBT

4,6-DM-HH-DBT and 4,6-DM-PH-DBT were prepared by hydrogenation of 4,6-DM-DBT under high hydrogen pressure in a 300-ml stainless steel autoclave. The autoclave was loaded with 10 g of 10 wt% Pd/C catalyst, 10 g of 4,6-DM-DBT, and 180 ml of glacial acetic acid (as solvent, crucial for a high conversion). The reaction was carried out at 200 °C and 15 MPa H_2 for 5 h. The hydrogenation product consisted of 47% 4,6-DM-DBT, 4% 4,6-DM-TH-DBT, 42% 4,6-DM-HH-DBT, 4% 4,6-DM-PH-DBT, and 3% desulfurized products.

After the autoclave was cooled to room temperature, the catalyst was filtered off. Because the catalyst adsorbed a large amount of products, it was refluxed in chloroform for 1 h and

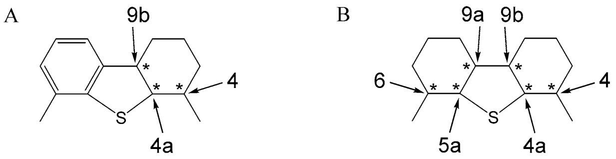

Scheme 1. Structure of 4,6-DM-HH-DBT (A) and 4,6-DM-PH-DBT (B) with their three and six chiral centers (*), respectively.

filtered a second time. Both filtrates were then evaporated separately to dryness, and the unreacted 4,6-DM-DBT was purified by recrystallization in toluene. The mother liquors were evaporated together with commercial silica, and the reaction products were separated twice by column chromatography, as was done in the preparation of 4,6-DM-TH-DBT. There were three different isomers of 4,6-DM-HH-DBT in the reaction mixture, isolated in the following proportions: 28% isomer A, 9% isomer B, and 63% isomer C. After recrystallization, these isomers were characterized by ^{1}H and ^{13}C NMR spectroscopy, MS/MS experiments, and X-ray crystal structure determination [23].

As illustrated in Scheme 1A, there are three chiral centers in 4,6-DM-HH-DBT. Thus the carbon atoms at positions 4, 4a, and 9b can have their hydrogen atom in either the *cis*- or the *trans*-configuration relative to each other, leading to four different diastereomers. Complete characterization of the 4,6-DM-HH-DBT isomers obtained from the hydrogenation reaction revealed that isomer A has the *(4,4a)-trans–(4a,9b)-cis* configuration, isomer B has the *(4,4a)-trans–(4a,9b)-trans* configuration, and isomer C has the *(4,4a)-cis–(4a,9b)-cis* configuration. The fourth diastereomer with the *(4,4a)-cis–(4a,9b)-trans* configuration (isomer D) was found in trace amounts among the reaction products, but in too small an amount to allow isolation for characterization. In the case of 4,6-DM-PH-DBT, the conditions led almost exclusively to the production of one diastereomer. ^{1}H and ^{13}C NMR spectroscopy showed that this had the *all-cis* configuration with respect to the six chiral centers of the molecule, located at positions 4, 4a, 5a, 6, 9a, and 9b (Scheme 1B).

3. Results

3.1. HDS of 4,6-DM-DBT

Fig. 1 shows the reaction profile and the product selectivities in the HDS of 4,6-DM-DBT over 50 mg of 0.50 wt% Pd/γ-Al$_2$O$_3$. At $\tau = 5$ g min/mol, the conversion reached 62%, demonstrating the very high activity of the noble metal catalyst. Under identical conditions (300 °C, 5 MPa total pressure, 1 kPa of 4,6-DM-DBT), but in the presence of 35 kPa H$_2$S, only 18% of 4,6-DM-DBT was converted at $\tau = 5$ g min/mol over 50 mg of sulfided NiMo/γ-Al$_2$O$_3$ catalyst, even though the metal loading was much higher with 8 wt% Mo and 3 wt% Ni [24].

During the reaction over the palladium catalyst, six species were observed: 3,3′-dimethyl-biphenyl (3,3′-DM-BP), the product of the DDS pathway, and 4,6-DM-TH-DBT, 4,6-DM-HH-DBT, 4,6-DM-PH-DBT, 3,3′-dimethyl-cyclohexylbenzene (3,3′-DM-CHB), and 3,3′-dimethyl-bicyclohexyl (3,3′-DM-BCH), the intermediate and final products of the HYD route. The results of GC-MS analysis confirmed that the tetrahydro-intermediate was 4,6-dimethyl-1,2,3,4-tetrahydro-dibenzothiophene, with the double bond located at the bridge between the partially hydrogenated six-member ring and the thiophene ring (the 4a and 9b positions in Scheme 1).

4,6-DM-TH-DBT, 4,6-DM-HH-DBT, and 4,6-DM-PH-DBT showed behavior typical of reaction intermediates, formed by (partial) hydrogenation of 4,6-DM-DBT. Their yields passed through a maximum and their selectivities decreased with weight time, which means that they were subsequently converted. The final products of the HYD pathway after further desulfurization were 3,3′-DM-CHB and 3,3′-DM-BCH, which showed continuously increasing yield and selectivity curves. The 3,3′-DM-BP selectivity was only 1% and was almost constant throughout the reaction. Therefore, the product of the DDS route did not seem to hydrogenate further to 3,3′-DM-CHB under our conditions; 99% of 4,6-DM-DBT was always converted via the HYD pathway, with only 1% converted through DDS.

At low weight time, 4,6-DM-TH-DBT was the most abundant product, and the sharp increase in its yield demonstrates that it formed rapidly. The three (partially) hydrogenated sulfur compounds represented 65% of the reaction products at short weight time ($\tau = 0.5$ g min/mol) and 17% even at high weight time ($\tau = 9$ g min/mol). This indicates that partial hydrogenation of 4,6-DM-DBT proceeded easily on Pd/γ-Al$_2$O$_3$, but that subsequent sulfur removal was relatively difficult. Moreover, the three (partially) hydrogenated sulfur compounds evolved at the same time, and their yields had similar time dependence. The ratio of 4,6-DM-TH-DBT to 4,6-DM-HH-DBT was con-

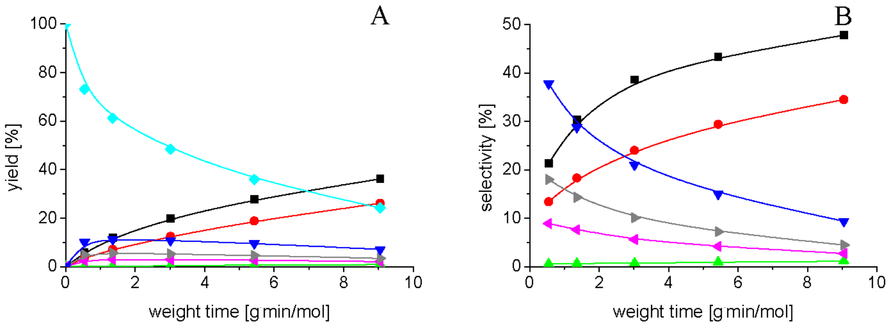

Fig. 1. Reaction profile (A) and product selectivities (B) in the HDS of 4,6-DM-DBT over 0.50 wt% Pd/γ-Al$_2$O$_3$ as a function of weight time (◆ 4,6-DM-DBT; ▲ 3,3′-DM-BP; ▼ 4,6-DM-TH-DBT; ► 4,6-DM-HH-DBT; ◄ 4,6-DM-PH-DBT; ● 3,3′-DM-CHB; ■ 3,3′-DM-BCH).

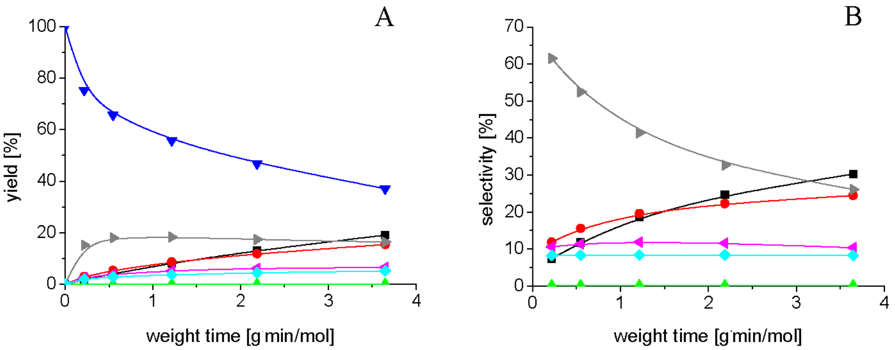

Fig. 2. Reaction profile (A) and product selectivities (B) in the HDS of 4,6-DM-TH-DBT over 0.50 wt% Pd/γ-Al_2O_3 as a function of weight time (◆ 4,6-DM-DBT; ▲ 3,3′-DM-BP; ▼ 4,6-DM-TH-DBT; ► 4,6-DM-HH-DBT; ◄ 4,6-DM-PH-DBT; ● 3,3′-DM-CHB; ■ 3,3′-DM-BCH).

stant and equal to 2.1 throughout the reaction, whereas the ratio of 4,6-DM-TH-DBT to 4,6-DM-PH-DBT changed from 4.2 to 3.4 with increasing weight time. At $\tau \geqslant 1.3$ g min/mol, the fully hydrogenated and desulfurized compound, 3,3′-DM-BCH, became the main reaction product; 3,3′-DM-CHB was the second most abundant component, at $\tau \geqslant 2.6$ g min/mol.

Assuming pseudo-first-order kinetics for the HDS of 4,6-DM-DBT at low conversions (where inhibition by H_2S is practically negligible), we calculated a rate constant of $k_{4,6\text{-DM-DBT}} = 0.58$ mol/(g min) for the disappearance of the reactant. Together with the selectivity of the pathways (1% DDS and 99% HYD), this gives the rate constants of the two routes: $k_{\text{DDS}} = 0.006$ mol/(g min) and $k_{\text{HYD}} = 0.57$ mol/(g min).

3.2. *HDS of 4,6-DM-TH-DBT*

The conversion of 4,6-DM-TH-DBT over 20 mg of 0.50 wt% Pd/γ-Al_2O_3 was about 10% higher than that of 4,6-DM-DBT over 50 mg of 0.50 wt% Pd/γ-Al_2O_3 under the same conditions (300 °C and 5 MPa). The reaction profile and product selectivities are shown in Fig. 2. The same species were observed as in the HDS of 4,6-DM-DBT. Up to $\tau = 3.2$ g min/mol, the main product was 4,6-DM-HH-DBT, showing the typical reaction profile of an intermediate. This compound forms rapidly by hydrogenation of the reactant, 4,6-DM-TH-DBT, and reacts further, as demonstrated by the (slow) decrease in its yield with weight time.

4,6-DM-DBT was obtained in significant amounts, with a constant selectivity of 8% throughout the reaction; it must be formed by dehydrogenation of the reactant on the catalyst surface. As a result of the formation of this compound, traces of 3,3′-DM-BP were also detected (yield $\leqslant 0.1\%$). The rate at which 4,6-DM-PH-DBT and 4,6-DM-DBT form must be slightly higher than the rate of consumption, because their yields increase slowly to 7 and 5%, respectively, at $\tau = 3.6$ g min/mol. Up to $\tau = 1.5$ g min/mol, larger amounts of 3,3′-DM-CHB were produced than of 3,3′-DM-BCH, whereas at high weight times the fully hydrogenated compound was the most abundant species.

From the conversion of 4,6-DM-TH-DBT at low weight time and the assumption of pseudo-first-order kinetics, we calculated a rate constant of $k_{4,6\text{-DM-TH-DBT}} = 1.30$ mol/(g min) for the disappearance of the reactant. 4,6-DM-TH-DBT reacts by hydrogenation to 4,6-DM-HH-DBT, 4,6-DM-PH-DBT, and their desulfurized products, 3,3′-DM-CHB and 3,3′-DM-BCH, and by dehydrogenation to 4,6-DM-DBT and the desulfurized 3,3′-DM-BP. Adding the selectivities of the components involved in these two reaction branches and extrapolating them to $\tau = 0$ provided initial selectivities of 92% for the hydrogenation and 8% for the dehydrogenation route. The hydrogenation of 4,6-DM-TH-DBT was thus 11.5 times faster than the dehydrogenation. Based on these values, the following rate constants were obtained for the two pathways: $k_{\text{hydrogenation}} = 1.19$ mol/(g min) and $k_{\text{dehydrogenation}} = 0.10$ mol/(g min).

3.3. *HDS of 4,6-DM-HH-DBT*

The 4,6-DM-HH-DBT reactant consisted of 88% isomer C, 11% isomer A, 1% isomer B, and traces of isomer D. To treat the experimental data, all of the isomer peaks were quantified separately and added together under the general name 4,6-DM-HH-DBT. The reaction profile shows that 4,6-DM-HH-DBT is a very reactive component under our operating conditions (Fig. 3). Half of it converted already at $\tau = 0.2$ g min/mol with a selectivity of 70% to 4,6-DM-TH-DBT. The latter molecule forms by dehydrogenation of the reactant and acts as a reaction intermediate. It was always the most abundant compound, having 40% selectivity at high weight time ($\tau = 3.6$ g min/mol). 4,6-DM-DBT was obtained as a product of subsequent dehydrogenation and showed a constant selectivity of 8% throughout the reaction. Trace amounts of 3,3′-DM-BP were also detected (yield $\leqslant 0.15\%$). The yields of 4,6-DM-PH-DBT and 4,6-DM-DBT increased progressively to 9 and 7% at $\tau = 3.6$ g min/mol, respectively; thus, their formation was always somewhat faster than their consumption. Among the desulfurized products, 3,3′-DM-BCH was more abundant than 3,3′-DM-CHB at $\tau \geqslant 1$ g min/mol.

Assuming pseudo-first-order kinetics, we obtained $k_{4,6\text{-DM-HH-DBT}} = 3.02$ mol/(g min) for the conversion of 4,6-DM-HH-DBT at low weight time. According to the reaction network, 4,6-DM-HH-DBT can convert in three different ways: by hydrogenation to 4,6-DM-PH-DBT and further desulfurization to 3,3′-DM-BCH; by dehydrogenation to 4,6-DM-TH-DBT, 4,6-DM-DBT, and the desulfurized 3,3′-DM-BP; and by direct sulfur removal to 3,3′-DM-CHB. Hence, the sums of the selectivities of the involved products in each branch

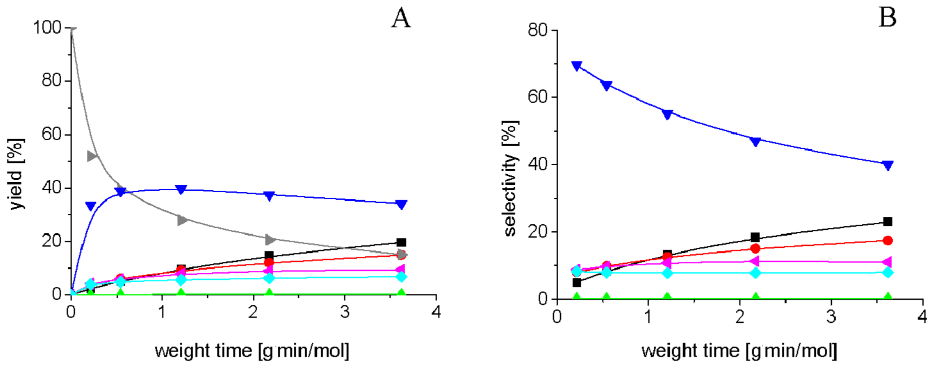

Fig. 3. Reaction profile (A) and product selectivities (B) in the HDS of 4,6-DM-HH-DBT over 0.50 wt% Pd/γ-Al_2O_3 as a function of weight time (◆ 4,6-DM-DBT; ▲ 3,3′-DM-BP; ▼4,6-DM-TH-DBT; ► 4,6-DM-HH-DBT; ◄ 4,6-DM-PH-DBT; ● 3,3′-DM-CHB; ■ 3,3′-DM-BCH).

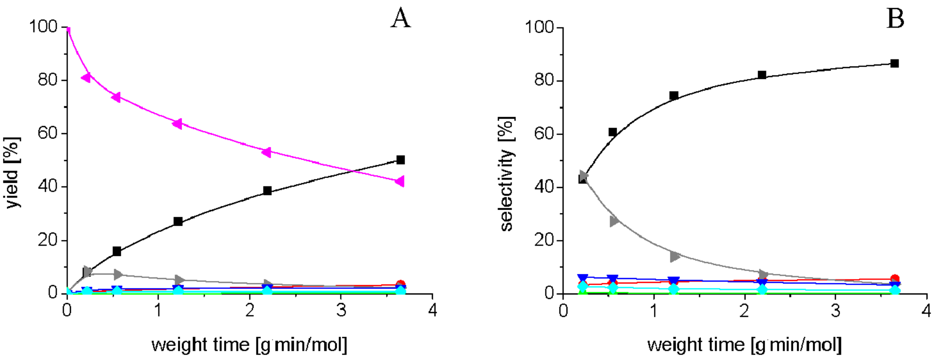

Fig. 4. Reaction profile (A) and product selectivities (B) in the HDS of 4,6-DM-PH-DBT over 0.50 wt% Pd/γ-Al_2O_3 as a function of weight time (◆ 4,6-DM-DBT; ▲ 3,3′-DM-BP; ▼ 4,6-DM-TH-DBT; ► 4,6-DM-HH-DBT; ◄ 4,6-DM-PH-DBT; ● 3,3′-DM-CHB; ■ 3,3′-DM-BCH).

and their extrapolation to $\tau = 0$ quantify the initial proportions of the three independent routes: 10% for hydrogenation, 83% for dehydrogenation, and 7% for desulfurization. These values demonstrate that 4,6-DM-HH-DBT reacts 8 times faster by dehydrogenation than by hydrogenation and 12 times faster by dehydrogenation than by direct sulfur removal. From the pathway selectivities, the following rate constants were calculated: $k_{\text{dehydrogenation}} = 2.51\ \text{mol}/(\text{g}\,\text{min})$, $k_{\text{hydrogenation}} = 0.30\ \text{mol}/(\text{g}\,\text{min})$, and $k_{\text{desulfurization}} = 0.21\ \text{mol}/(\text{g}\,\text{min})$.

3.4. HDS of 4,6-DM-PH-DBT

The starting material, 4,6-DM-PH-DBT, contained 86% of the *all-cis* diastereomer and small amounts of other isomers. During the HDS reaction over 20 mg of 0.50 wt% Pd/γ-Al_2O_3, isomerization of the reactant occurred at the same time as its conversion; more than 10 different diastereomers were detected. These were quantified separately, but the plotted yield of 4,6-DM-PH-DBT represents the sum of all the isomers. The experimental results are given in Fig. 4.

4,6-DM-PH-DBT did not seem to be particularly reactive under our experimental conditions. At $\tau = 0.2\ \text{g}\,\text{min/mol}$, it converted mainly (with 90% selectivity) to equal amounts of 4,6-DM-HH-DBT by dehydrogenation and of 3,3′-DM-BCH by desulfurization. 4,6-DM-HH-DBT acted as a reaction intermediate. It was formed rapidly at low weight time but transformed easily, as shown by the rather fast decrease in its yield and selectivity curves. The dehydrogenation intermediate 4,6-DM-TH-DBT was also observed in low amounts, with a maximum yield of 2% and a constantly decreasing selectivity. 4,6-DM-DBT and its desulfurization product 3,3′-DM-BP were obtained in trace amounts (0.7 and 0.1%, respectively). Above $\tau = 0.2\ \text{g}\,\text{min/mol}$, the major product was 3,3′-DM-BCH, formed directly by desulfurization of the reactant, 4,6-DM-PH-DBT. Its high selectivity of 43% at $\tau = 0.2\ \text{g}\,\text{min/mol}$ doubled to 87% at $\tau = 3.7\ \text{g}\,\text{min/mol}$. Small amounts of the desulfurized product 3,3′-DM-CHB formed with continuously increasing yield and selectivity. At high weight time ($\tau \geqslant 2.9\ \text{g}\,\text{min/mol}$), it was the second most abundant reaction product.

Pseudo-first-order kinetics led to a rate constant of $k_{\text{4,6-DM-PH-DBT}} = 0.96\ \text{mol}/(\text{g}\,\text{min})$ for the disappearance of 4,6-DM-PH-DBT at low weight time. Two different reaction routes are possible for 4,6-DM-PH-DBT: direct sulfur removal to produce 3,3′-DM-BCH and dehydrogenation to 4,6-DM-HH-DBT, 4,6-DM-TH-DBT, 4,6-DM-DBT, and the desulfurized products 3,3′-DM-CHB and 3,3′-DM-BP. The ratio of all of the products involved in the dehydrogenation branch to 3,3′-DM-BCH corresponded to the ratio of the two reaction pathways. Its extrapolation to $\tau = 0$ gave a value of about 3 for the initial ratio of the dehydrogenation to the desulfurization route. In other words, 75% of 4,6-DM-PH-DBT converted initially by dehydrogenation, whereas only 25% was directly desulfurized. Therefore, the rate constants of these pathways are estimated as $k_{\text{dehydrogenation}} = 0.72\ \text{mol}/(\text{g}\,\text{min})$ and $k_{\text{desulfurization}} = 0.24\ \text{mol}/(\text{g}\,\text{min})$.

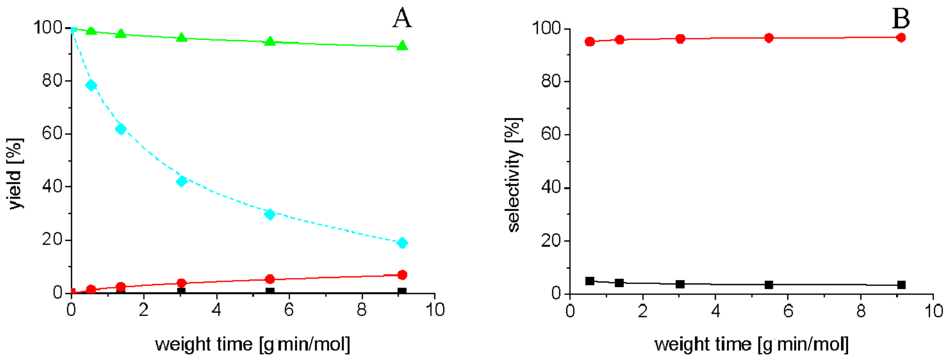

Fig. 5. Reaction profile (A) and product selectivities (B) in the hydrogenation of 3,3′-DM-BP in the presence of DBT over 0.50 wt% Pd/γ-Al_2O_3 as a function of weight time (◆ DBT; ▲ 3,3′-DM-BP; ● 3,3′-DM-CHB; ■ 3,3′-DM-BCH).

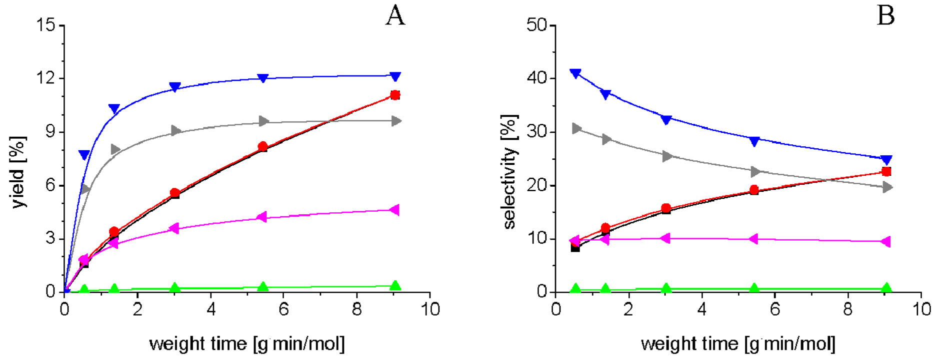

Fig. 6. Product yields (A) and selectivities (B) in the HDS of 4,6-DM-DBT at 280 °C over 0.50 wt% Pd/γ-Al_2O_3 as a function of weight time (▲ 3,3′-DM-BP; ▼ 4,6-DM-TH-DBT; ► 4,6-DM-HH-DBT; ◄ 4,6-DM-PH-DBT; ● 3,3′-DM-CHB; ■ 3,3′-DM-BCH).

3.5. *Hydrogenation of 3,3′-DM-BP*

To investigate the possible hydrogenation of the desulfurized reaction products, hydrogenation of 1 kPa 3,3′-DM-BP was performed at 300 °C and 5 MPa total pressure over 50 mg of 0.50 wt% Pd/γ-Al_2O_3. The experiment was carried out simultaneously with the HDS of 1 kPa of DBT, to simulate the presence of sulfur compounds in the system. Fig. 5 shows the reaction profiles with the concentrations of DBT (dashed line) and 3,3′-DM-BP, the yields of 3,3′-DM-CHB and 3,3′-DM-BCH, as well as the product selectivities for the hydrogenation of 3,3′-DM-BP. Very slow conversion of 3,3′-DM-BP was observed in the presence of the sulfur-containing DBT. At $\tau = 9$ g min/mol, when only 19% DBT remains, the conversion of 3,3′-DM-BP barely reached 7%. The hydrogenation occurred almost exclusively to 3,3′-DM-CHB, with a selectivity of 97%. The fully hydrogenated component, 3,3′-DM-BCH, formed in small quantities only, meaning that the subsequent hydrogenation would be more difficult, as was expected.

3.6. *Effect of the temperature on the HDS of 4,6-DM-DBT*

The effect of temperature on the HDS of 4,6-DM-DBT was studied by carrying out an experiment over 50 mg of 0.50 wt% Pd/γ-Al_2O_3 at 280 °C and 5 MPa total pressure. The yields and selectivities of the different reaction products at this lower temperature show that 4,6-DM-TH-DBT was the major product throughout the reaction, with a high selectivity of 41% at $\tau = 0.5$ g min/mol and 25% at $\tau = 9$ g min/mol (Fig. 6). 4,6-DM-HH-DBT was the second most abundant reaction product up to $\tau = 7.3$ g min/mol. The yields of 4,6-DM-TH-DBT and 4,6-DM-HH-DBT both increased sharply initially and then leveled off; they had a constant ratio of 1.3. The third hydrogenated sulfur compound, 4,6-DM-PH-DBT, behaved slightly differently, showing a constant selectivity at 10% and a steadily increasing yield. Its formation was stronger than its consumption throughout the reaction. The ratio of 4,6-DM-TH-DBT to 4,6-DM-PH-DBT decreased from 4.3 to 2.6 with increasing weight time.

The three (partially) hydrogenated sulfur compounds always constituted the major part of the reaction products at 280 °C. The sum of their selectivities amounted to 82% at $\tau = 0.5$ g min/mol and was still 54% at $\tau = 9$ g min/mol. This indicates that the subsequent sulfur removal is more difficult than the partial hydrogenation of 4,6-DM-DBT, which is relatively fast on Pd/γ-Al_2O_3. The final desulfurized products, 3,3′-DM-CHB and 3,3′-DM-BCH, showed about the same steady increase in yield and selectivity at rather low levels. The product of the DDS pathway, 3,3′-DM-BP, formed in trace amounts and had a constant selectivity of 0.6%. Therefore, the ratio of the DDS to HYD route was 0.6 to 99.4 for the conversion of 4,6-DM-DBT at 280 °C.

4. Discussion

4.1. *Reaction network of the HDS of 4,6-DM-DBT*

The hydrodesulfurization of 4,6-DM-DBT and its (partially) hydrogenated sulfur-containing intermediates at 300 °C and 5 MPa total pressure over 0.50 wt% Pd/γ-Al_2O_3 shows that the desulfurized molecules, 3,3′-dimethyl-cyclohexylbenzene and 3,3′-dimethyl-bicyclohexyl, were final products of the HYD pathway, because their yields and selectivities increased steadily as a function of weight time (Figs. 1–4). In turn, 3,3′-dimethyl-biphenyl was the only product of the DDS route. The partially and fully hydrogenated sulfur-containing compounds formed easily and acted as reaction intermediates, with their yields passing through a maximum (Fig. 1). As expected, 4,6-DM-TH-DBT was the primary product of the HYD pathway. Surprisingly, 4,6-DM-HH-DBT also seemed to have nonzero selectivity at $\tau = 0$, even though it is a secondary product according to Scheme 2. This would mean that it behaves as a primary product as well. Moreover, 4,6-DM-TH-DBT and 4,6-DM-HH-DBT evolved at the same time with a constant ratio of 2.1, suggesting that they were in equilibrium under the present conditions and that the transformation of 4,6-DM-TH-DBT to 4,6-DM-HH-DBT was rapid relative to the other reactions. If this transformation were much faster than the formation of 4,6-DM-TH-DBT, then 4,6-DM-HH-DBT would appear to be a primary product as well. Furthermore, slow diffusion out of the catalyst pores may mask the true kinetic character of the intermediates. The behavior of 4,6-DM-PH-DBT was less clear, because the slope of its selectivity curve was much less steep at low weight time. According to the chemistry, 4,6-DM-PH-DBT should be a tertiary product.

The experiments performed with the different sulfur-containing intermediates as reactants show that under our operating conditions, hydrogenation and dehydrogenation reactions occurred easily on the catalyst surface. All of the sulfur compounds, even 4,6-DM-DBT, were always visible, and significant amounts were produced rapidly. The HDS of 4,6-DM-TH-DBT showed that 4,6-DM-HH-DBT was a primary product that formed rapidly (Fig. 2). This explains why it behaved like a primary product in the HDS of 4,6-DM-DBT. 4,6-DM-HH-DBT acted as an intermediate, but its effective disappearance was rather slow. The ratio of 4,6-DM-TH-DBT to 4,6-DM-HH-DBT decreased with weight time and reached 2.3 at $\tau = 3.6$ g min/mol. Both 4,6-DM-DBT and 4,6-DM-PH-DBT had almost flat selectivity curves, although the former is expected to be a primary product and the latter a secondary product. Furthermore, 3,3′-DM-CHB seemed to have nonzero selectivity by extrapolation to $\tau = 0$. This can be explained by the fact that if there is fast equilibrium between 4,6-DM-TH-DBT and 4,6-DM-HH-DBT, then 4,6-DM-PH-DBT and 3,3′-DM-CHB will behave as (quasi) primary products. Thus, their selectivities start with nonzero values at $\tau = 0$.

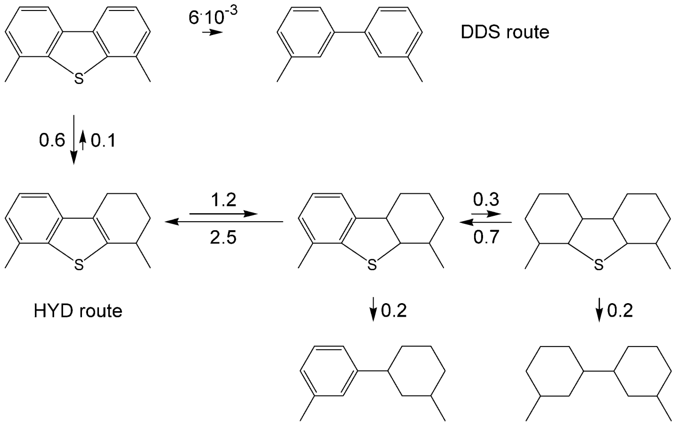

Scheme 2. Reaction network and semiquantitative pseudo-first-order rate constants in the HDS of 4,6-DM-DBT at 300 °C and 5 MPa over 0.50 wt% Pd/γ-Al_2O_3.

In the HDS of 4,6-DM-HH-DBT, large amounts of 4,6-DM-TH-DBT formed very rapidly by dehydrogenation of the reactant, with 4,6-DM-TH-DBT clearly a primary product (Fig. 3). The relative concentrations of 4,6-DM-TH-DBT and 4,6-DM-HH-DBT at high weight time were very similar to those obtained in the HDS of 4,6-DM-TH-DBT. At $\tau = 3.6$ g min/mol, their ratio equaled 1.8. Furthermore, 3,3′-DM-CHB and 3,3′-DM-BCH had the same yields (15 and 19%, respectively) starting from 4,6-DM-TH-DBT and 4,6-DM-HH-DBT. These values are very close to the 14 and 22% obtained at $\tau = 3.6$ g min/mol in the HDS of 4,6-DM-DBT. In the reaction of 4,6-DM-HH-DBT, 4,6-DM-PH-DBT and 3,3′-DM-CHB acted as primary products, with their nonzero selectivities obtained by extrapolation to $\tau = 0$. 4,6-DM-DBT should be a secondary product, but it behaves like a primary product, probably because of the fast equilibrium between 4,6-DM-TH-DBT and 4,6-DM-HH-DBT.

The HDS of 4,6-DM-PH-DBT showed that 4,6-DM-HH-DBT and 3,3′-DM-BCH are primary products, because their selectivities have nonzero values by extrapolation to $\tau = 0$ (Fig. 4). As mentioned earlier, 4,6-DM-PH-DBT reacted approximately three times faster by dehydrogenation than by desulfurization. In contrast to the experiments in which 4,6-DM-TH-DBT and 4,6-DM-HH-DBT were used as reactants, in the HDS of 4,6-DM-PH-DBT, the sulfur-containing products (4,6-DM-HH-DBT, 4,6-DM-TH-DBT, and 4,6-DM-DBT) formed in much smaller amounts. Even 4,6-DM-HH-DBT reached a maximum yield of only 8%. This may be due to the fact that the rate constant for hydrogenation of 4,6-DM-HH-DBT to 4,6-DM-PH-DBT was slightly higher than that for desulfurization of 4,6-DM-HH-DBT, making desulfurization proceed mainly through 4,6-DM-PH-DBT.

The fast hydrogenation and dehydrogenation reactions of the partially hydrogenated sulfur-containing compounds and their more or less parallel evolution suggest that 4,6-DM-TH-DBT and 4,6-DM-HH-DBT were close to equilibrium. Fig. 7A illustrates the ratio between those two components during the different HDS experiments. As mentioned earlier, their ratio in the HDS of 4,6-DM-DBT at 300 °C remained constant at 2.1. In the experiments performed with the partially hydrogenated sulfur intermediates, 4,6-DM-TH-DBT and 4,6-DM-HH-DBT, the ratio approached 2.1. The ratio of 4,6-DM-TH-DBT to 4,6-DM-HH-DBT in the HDS of 4,6-DM-PH-DBT started at 0

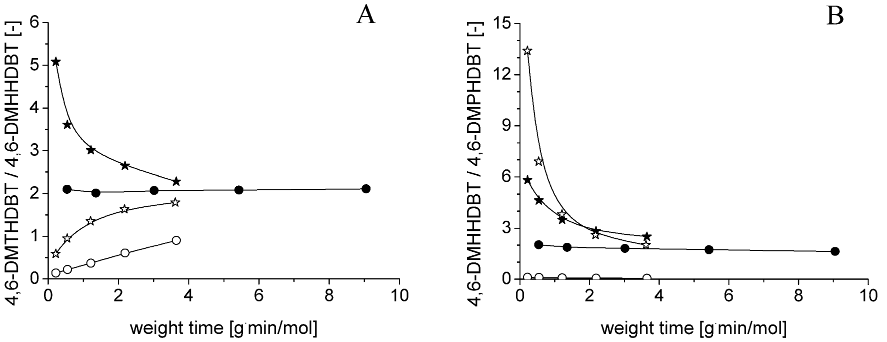

Fig. 7. Ratio of 4,6-DM-TH-DBT to 4,6-DM-HH-DBT (A) and ratio of 4,6-DM-HH-DBT to 4,6-DM-PH-DBT (B) obtained in the HDS of 4,6-DM-DBT (●), 4,6-DM-TH-DBT (★), 4,6-DM-HH-DBT (☆), and 4,6-DM-PH-DBT (○) at 300 °C over 0.50 wt% Pd/γ-Al_2O_3 as a function of weight time.

for $\tau = 0$, because 4,6-DM-TH-DBT was not present in the system at the beginning of the reaction. Thereafter it increased with weight time, as the partially hydrogenated sulfur-containing compounds form progressively. The increase was slow, however, and the ratio was far from equilibrium. This might be due to inhibition by H_2S produced during the reaction. Also, the diastereomer of 4,6-DM-PH-DBT, used at the start of the experiment, isomerized very rapidly to many other isomers. Thus the reactivity determined from the data obtained at low conversion may not represent the system at high weight time.

Fig. 7B shows the ratio of 4,6-DM-HH-DBT to 4,6-DM-PH-DBT in the HDS reactions of 4,6-DM-DBT, 4,6-DM-TH-DBT, 4,6-DM-HH-DBT, and 4,6-DM-PH-DBT. The ratio obtained in the HDS of 4,6-DM-DBT at 300 °C decreased slightly from 2.0 to 1.6 with weight time. In the HDS of 4,6-DM-TH-DBT and 4,6-DM-HH-DBT, the 4,6-DM-HH-DBT to 4,6-DM-PH-DBT ratio decreased strongly with time, reaching 2.5 and 2.0, respectively, at $\tau = 3.6$ g min/mol. The three curves tended to take the same direction, but equilibrium apparently had not yet been reached. Starting the HDS reaction with 4,6-DM-PH-DBT led to a very small, even slightly decreasing ratio. The low ratio is probably due to the continuous excess of 4,6-DM-PH-DBT, as a result of the rather low rates of hydrogenation and dehydrogenation between 4,6-DM-HH-DBT and 4,6-DM-PH-DBT.

4.2. *Reaction rates*

Comparing the conversions of the different sulfur-containing compounds, 4,6-DM-HH-DBT appears to be the most reactive molecule (Figs. 1–4). However, the high reactivity of 4,6-DM-HH-DBT is due mainly to its fast dehydrogenation to 4,6-DM-TH-DBT (70% selectivity at $\tau = 0.2$ g min/mol). Therefore, one must compare the rate constants for the separate reaction steps (Scheme 2) to learn more about the rates of desulfurization. The pseudo-first-order rate constants for the direct removal of sulfur from the different sulfur-containing components show that desulfurizing 4,6-DM-DBT was extremely difficult ($k_{\mathrm{DDS}} = 0.006$ mol/(g min)), whereas 4,6-DM-HH-DBT and 4,6-DM-PH-DBT had fast and almost similar reactivities ($k_{\mathrm{DDS}} = 0.21$ mol/(g min) and 0.24 mol/(g min), respectively). This reactivity order for the removal of sulfur, 4,6-DM-DBT $\ll$ 4,6-DM-HH-DBT $\approx$ 4,6-DM-PH-DBT, demonstrates that a higher saturation degree of the molecules helps decrease the steric hindrance of the methyl groups located at positions 4 and 6 [25]. As a result, the hydrogenated ring can adopt a chair conformation, which moves the bulky substituent away from the sulfur atom, making the sulfur atom more accessible for desulfurization. Furthermore, molecular modeling calculations indicate that the lengths of the C–S bonds increase with the saturation degree of the molecules, making them more reactive.

The hydrogenation and dehydrogenation rate constants were several times larger than the desulfurization rate constants (Scheme 2). The largest rate constants were for the reactions between 4,6-DM-TH-DBT and 4,6-DM-HH-DBT, and the lowest rate constant was for the dehydrogenation of 4,6-DM-TH-DBT to 4,6-DM-DBT. These differences must be due to conformation of the reacting molecules on the catalyst surface.

The conversion of the sulfur-containing compounds to desulfurized products (defined as HDS conversion) as a function of weight time again shows that 4,6-DM-PH-DBT behaves differently than the other sulfur-containing molecules. 4,6-DM-DBT, 4,6-DM-TH-DBT, and 4,6-DM-HH-DBT had similar HDS conversions (about 35% at $\tau = 3.6$ g min/mol), demonstrating that the reactant desulfurization must go through 4,6-DM-HH-DBT almost exclusively and that the consecutive hydrogenation reactions are not rate-limiting. Otherwise, depending on the starting sulfur-containing component, different HDS conversions would be obtained. In contrast, 4,6-DM-PH-DBT had a higher desulfurization conversion of 53% at $\tau = 3.6$ g min/mol, with an HDS selectivity to 3,3′-DM-BCH of 94%. This confirms that it is easy to remove sulfur directly, with only a minor contribution of the dehydrogenation route.

Assuming that equilibrium between 4,6-DM-TH-DBT and 4,6-DM-HH-DBT is established, the product selectivities obtained from their HDS experiments can be recalculated by treating both partially hydrogenated sulfur compounds together as reactants. The resulting product selectivity curves of the HDS of 4,6-DM-TH-DBT and 4,6-DM-HH-DBT were similar (Fig. 8) and indicate that equilibrium between these two molecules was almost reached. 4,6-DM-DBT and 4,6-DM-PH-DBT now clearly behaved as primary products, formed by dehydrogenation of 4,6-DM-TH-DBT and hydrogenation of 4,6-DM-HH-DBT, respectively. The selectivities of 4,6-DM-DBT and 4,6-DM-PH-DBT decreased with weight time, demonstrating that they are reaction intermediates that are subsequently converted.

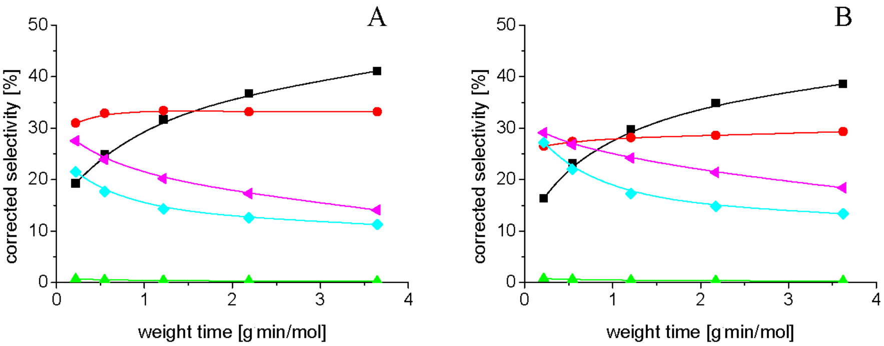

Fig. 8. Corrected product selectivities in the HDS of 4,6-DM-TH-DBT (A) and in the HDS of 4,6-DM-HH-DBT (B) over 0.50 wt% Pd/γ-Al_2O_3 as a function of weight time, assuming equilibrium between 4,6-DM-TH-DBT and 4,6-DM-HH-DBT (◆ 4,6-DM-DBT; ◀ 4,6-DM-PH-DBT; ● 3,3′-DM-CHB; ■ 3,3′-DM-BCH; ▲ 3,3′-DM-BP).

3,3′-DM-CHB is also a primary product of the reaction network from the couple 4,6-DM-TH-DBT and 4,6-DM-HH-DBT. Its almost constant selectivity shows that this component is a final product (from the desulfurization of 4,6-DM-HH-DBT) that does not react further. The tendency of the selectivity of 3,3′-DM-BCH to reach zero by extrapolation to $\tau = 0$ confirms that it is a secondary product, formed by subsequent desulfurization of 4,6-DM-PH-DBT.

Studying the hydrogenation of 3,3′-dimethyl-biphenyl (the product of the DDS pathway in the HDS of 4,6-DM-DBT), performed in the presence of dibenzothiophene, showed that the hydrogenation reaction to 3,3′-DM-CHB was minor (Fig. 5) and that the subsequent hydrogenation of 3,3′-DM-CHB to 3,3′-DM-BCH was negligible. This confirms the observations made in previous experiments, in which continuously increasing yields and constant selectivities to 3,3′-DM-BP demonstrated that a significant reaction does not occur thereafter. This is especially understandable given the low concentrations of 3,3′-DM-BP in the system.

Combining the results leads to the reaction network in Scheme 2 for the HDS of 4,6-DM-DBT at 300 °C and 5 MPa over 0.50 wt% Pd/γ-Al_2O_3. In addition to the indicated reactions, direct desulfurization of 4,6-DM-TH-DBT also may be possible, as for 4,6-DM-DBT. This would yield 3,3′-DM-CHB, and finally 3,3-DM-CHB by further hydrogenation. However, this additional intermediate was not observed in the product mixture, probably because its formation is rather slow (probably as slow as the formation of 3,3′-dimethyl-biphenyl from 4,6-DM-DBT) and its hydrogenation is very fast.

The comparison of the semiquantitative pseudo-first-order rate constants emphasizes the fact that the desulfurization reactions, as well as the dehydrogenation of 4,6-DM-TH-DBT to 4,6-DM-DBT, are the slowest steps in the network. This explains the large proportions of all of the sulfur-containing intermediates under our experimental conditions. According to the reaction network and the rate constants estimated from the initial rates, 3,3′-DM-CHB should be present in larger amounts than 3,3′-DM-BCH at high weight time. Indeed, at equilibrium, the ratio of 4,6-DM-HH-DBT to 4,6-DM-PH-DBT should reach 2.4. Because the direct removal of sulfur is almost as fast from these two sulfur-containing molecules, about the same ratio, 2.4, should be found between their desulfurized products, 3,3′-DM-CHB and 3,3′-DM-BCH. However, in all of the experiments starting with different sulfur-containing compounds, 3,3′-DM-BCH was the most abundant desulfurized component for $\tau > 1$–1.5 g min/mol. This may be due to the fact that the rate constants considered were determined from experiments with specific diastereomers of 4,6-DM-HH-DBT (mainly *cis–cis*) and 4,6-DM-PH-DBT (*all-cis*). The reaction mixtures in actual systems may behave differently, especially because of isomerization. This is likely the case for 4,6-DM-PH-DBT, because only small amounts of the *all-cis* diastereomer were found under our experimental conditions. Another reason may be inhibition by H_2S produced during the reaction.

4.3. *Stereoisomers*

To treat the experimental data, all the isomers of the compounds formed during reaction were quantified separately and then added together. Four different diastereomers of 4,6-DM-HH-DBT and 13 of 4,6-DM-PH-DBT were detected. The HDS reactions of these sulfur-containing components indicate that the molecules used as reactants isomerized at the same time as their conversion. Therefore, plotting the selectivities of the isomers as a function of weight time may provide information about their relative behavior.

Fig. 9 illustrates the yields and the distribution of the 4,6-DM-HH-DBT diastereomers. The starting material contains 88% isomer C, 11% isomer A, 1% isomer B, and traces of isomer D. Fig. 9A indicates that the major isomer (C) converts rapidly and is almost the only reacting species. The yield of isomer A increases from 10 to 13% at low weight time, then decreases very slowly. The yield curves of the two other isomers (B and D) change only slightly and pass through a maximum at about $\tau = 2$ g min/mol. This suggests that isomerization occurs between the different diastereomers, but much more slowly than the overall conversion. Fig. 9B shows the changes in isomer distribution in the mixture during the HDS reaction. At the highest weight time in our experiment ($\tau = 3.6$ g min/mol), equilibrium was not reached, but the changes in the selectivities became smaller. At this point, the four diastereomers were present in the following proportions: 39% isomer C, 50% isomer A, 9% isomer B, and 2% isomer D. This sequence is in relatively good agreement with the energy estimations for the different

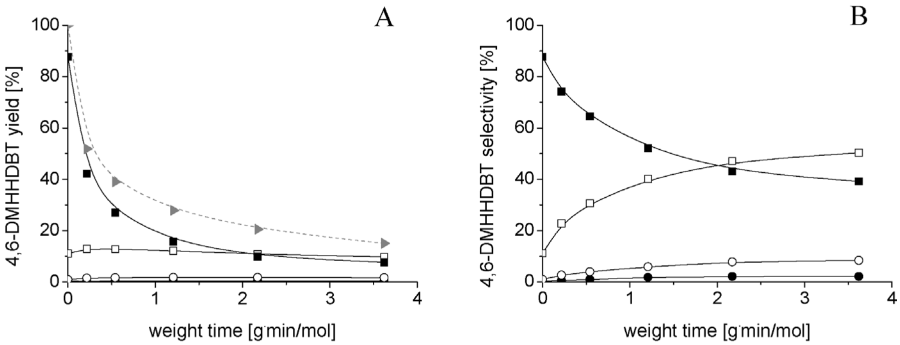

Fig. 9. Yields (A) and distribution (B) of diastereomers in the HDS of 4,6-DM-HH-DBT over 0.50 wt% Pd/γ-Al_2O_3 as a function of weight time (☐ isomer A; ○ isomer B; ■ isomer C; ● isomer D; ► overall concentration).

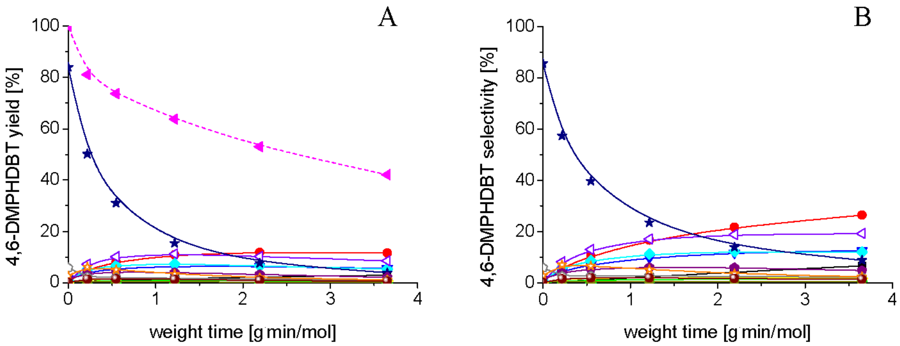

Fig. 10. Yields (A) and distribution (B) of diastereomers in the HDS of 4,6-DM-PH-DBT over 0.50 wt% Pd/γ-Al_2O_3 as a function of weight time (dashed line for the overall concentration) (★ *all-cis* 4,6-DM-PH-DBT, the other symbols denote other, not identified, isomers of 4,6-DM-PH-DBT).

diastereomers obtained by molecular modeling with the Hyperchem program. The molecular modeling indicates that isomers C (*cis–cis*) and A (*trans–cis*) are very close in energy (20.59 and 20.57 kcal/mol, respectively). They are the most stable species, followed by isomer B (*trans–trans*, 22.40 kcal/mol) and finally by isomer D (*cis–trans*, 24.41 kcal/mol), the configuration with the highest energy.

Similar treatment of the data for the HDS of 4,6-DM-PH-DBT led to the yields and the distribution of diastereomers depicted in Fig. 10. This situation is much more complex, because 13 species (of a maximum of 20 possible isomers) were detected, some present in only trace amounts. Only the major diastereomer of the starting mixture could be isolated and fully characterized; this appears to be the *all-cis* isomer. The yield curves confirm that the major diastereomer in the initial solution isomerized rapidly, because its disappearance (50% at $\tau = 0.2$ g min/mol) was much faster than the overall conversion (19% at $\tau = 0.2$ g min/mol). Most of the isomers produced have yields passing through a maximum at relatively low weight time, which means that they also react further.

The major 4,6-DM-HH-DBT diastereomer, produced in the HDS of 4,6-DM-PH-DBT throughout the experiment, was isomer A (*trans–cis*), not isomer C (*cis–cis*) as would be expected from the dehydrogenation of the *all-cis* 4,6-DM-PH-DBT diastereomer. This is probably due to the isomerization reactions. Moreover, the distribution of the 4,6-DM-HH-DBT diastereomers confirmed that isomer A is the isomer that converts most easily. In the same way, the *all-cis* 4,6-DM-PH-DBT diastereomer was only a minor product in the HDS of 4,6-DM-HH-DBT, which initially consisted mainly of isomer C (*cis–cis*).

Different isomers must also be considered in the case of the desulfurized products, because 3,3′-DM-CHB and 3,3′-DM-BCH have two and four chiral atoms, respectively. For 3,3′-DM-CHB, the two possible diastereomers were observed; these always had a ratio of about 1:1. Only three of the six possible diastereomers of 3,3′-DM-BCH were detected; their ratio was constant at 2:1:1. There were no significant changes in the isomer ratios when the reactions were started with the different sulfur-containing molecules or with 3,3′-DM-BP. It seems that the removal and reintroduction of a hydrogen atom from and to the sulfur-containing intermediates is fast on the Pd surface.

4.4. *Effect of temperature*

Comparing the results of the 4,6-DM-DBT HDS experiments performed at 300 °C and 280 °C (Figs. 1 and 6) shows that much smaller amounts of the desulfurized products formed at low temperature. Thus, the yields of 3,3′-DM-BP, 3,3′-DM-CHB, and 3,3′-DM-BCH decreased by factors of 2.0, 2.3, and 3.5, respectively, when the temperature was lowered by 20 °C. In contrast, the sulfur intermediates 4,6-DM-TH-DBT, 4,6-DM-HH-DBT, and 4,6-DM-PH-DBT gave even higher yields at 280 °C for $\tau > 3$ g min/mol. However, the shape of their curves at 280 °C differed; after a sharp increase at low weight time, the yields leveled off slowly. The maximum values were not yet reached, which means that the formation of the sulfur-containing intermediates by hydrogenation still predominated

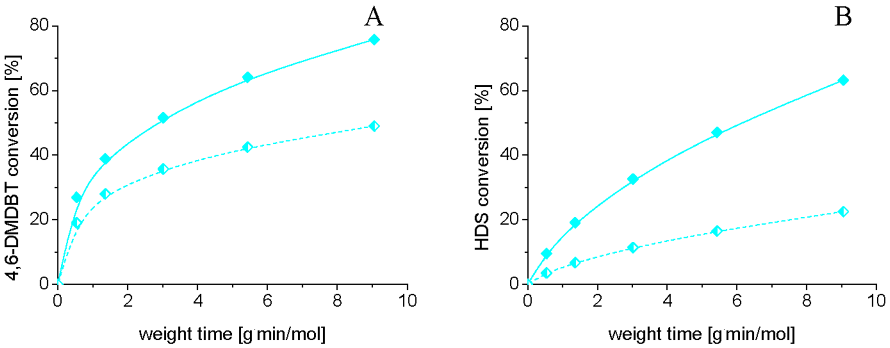

Fig. 11. Overall conversion (A) and HDS conversion (B) in the HDS of 4,6-DM-DBT at 300 °C (◆, solid line) and 280 °C (⬖, dashed line) over 0.50 wt% Pd/γ-Al_2O_3 as a function of weight time.

over their consumption by desulfurization. Fig. 11 confirms that desulfurization was more affected than hydrogenation by a change in the temperature, probably because desulfurization has a higher activation energy. When the temperature was lowered by 20 °C, the overall conversion of 4,6-DM-DBT decreased from 76 to 49% (Fig. 11A), whereas the HDS conversion, the conversion to desulfurized products, decreased from 63 to 23% (Fig. 11B) for $\tau = 9\ \mathrm{g\,min/mol}$. In other words, 83% of the converted molecules were desulfurized at 300 °C, but only 46% were desulfurized at 280 °C.

Moreover, the selectivity of the DDS route changed from 1 to 0.6% when the temperature was lowered by 20 °C, confirming that desulfurization is more strongly suppressed than hydrogenation at low temperature. The stronger promotional effect of temperature on the DDS pathway in the removal of sulfur from DBT [20,26] and 4,6-DM-DBT [24] was also observed on sulfided Co–Mo and Ni–Mo catalysts. The weaker effect of temperature on hydrogenation may also be explained by the fact that at lower temperature, the hydrogenation–dehydrogenation equilibrium shifts to the hydrogenation side. Fig. 12 confirms this point; the ratio of 4,6-DM-TH-DBT to 4,6-DM-HH-DBT (circles) was constant at 1.3 at 280 °C and at 2.1 at 300 °C.

As mentioned in Section 3.6, 4,6-DM-PH-DBT behaved differently at 280 °C than at 300 °C. Its evolution no longer followed that of the other two sulfur-containing intermediates, 4,6-DM-TH-DBT and 4,6-DM-HH-DBT. Fig. 12 illustrates this fact; at 300 °C, the ratio of 4,6-DM-HH-DBT to 4,6-DM-PH-DBT was not constant, but decreased slowly from 2.0 to 1.6 with increasing weight time. At 280 °C, the decrease from 3.2 to 2.1 was much more pronounced, demonstrated that equilibrium had not yet been reached. Moreover, the ratio of 4,6-DM-HH-DBT to 4,6-DM-PH-DBT was higher at 280 °C than at 300 °C. This demonstrates that the system was still in the kinetic regime and not under thermodynamic control.

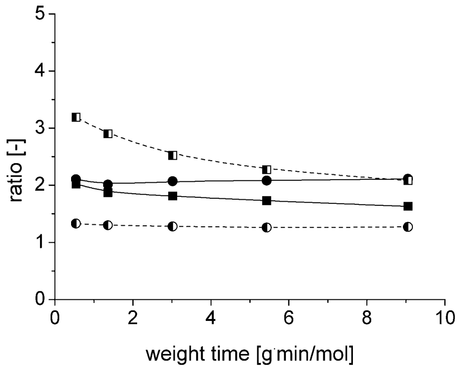

Fig. 12. Ratio of 4,6-DM-TH-DBT to 4,6-DM-HH-DBT (●, ◐) and ratio of 4,6-DM-HH-DBT to 4,6-DM-PH-DBT (■, ◧) at 300 °C (—) and 280 °C (- - -) in the HDS of 4,6-DM-DBT over 0.50 wt% Pd/γ-Al_2O_3 as a function of weight time.

5. Conclusions

A detailed study of the HDS reaction network of 4,6-dimethyl-dibenzothiophene was carried out over Pd/γ-Al_2O_3. The results indicate that 4,6-DM-DBT reacted almost exclusively through the hydrogenation pathway. The reactant was converted with only 1% selectivity via the direct desulfurization route. No significant further hydrogenation of the desulfurized compounds occurred under the experimental conditions.

All of the (partially) hydrogenated sulfur-containing intermediates of the HYD pathway—namely 4,6-DM-TH-DBT, 4,6-DM-HH-DBT, and 4,6-DM-PH-DBT—were observed in the HDS of 4,6-DM-DBT. After these three compounds were synthesized, the HDS experiments were performed separately. The results demonstrate that hydrogenation and dehydrogenation between the sulfur-containing intermediates occurred easily on the catalyst surface. Moreover, 4,6-DM-TH-DBT and 4,6-DM-HH-DBT rapidly converted to one another, due to their similar behavior and evolution. Calculations of their molar ratios confirmed that they were in equilibrium in the HDS of 4,6-DM-DBT and close to equilibrium in the experiments starting from the partially hydrogenated sulfur-containing compounds.

A comparison of the experimental data indicated that desulfurization was easier from the more saturated components. This confirms that the molecular planarity must be removed to weaken the steric hindrance caused by the methyl groups and to provide better access to the sulfur atom. Finally, temperature was found to have a stronger promotional effect on desulfurization than on hydrogenation. Thus, the direct desulfurization route and the removal of sulfur from the reaction intermediates were enhanced at higher temperature. Furthermore, the equilibrium between 4,6-DM-TH-DBT and 4,6-DM-HH-DBT shifted toward the 4,6-DM-TH-DBT side.

Acknowledgments

The authors thank Pavel Kukula, Vlastimil Cizek, and Marina Egorova for preparing the (partially) hydrogenated 4,6-dimethyl-dibenzothiophene derivatives.

References

[1] M.J. Girgis, B.C. Gates, Ind. Eng. Chem. Res. 30 (1991) 2021.
[2] D.D. Whitehurst, T. Isoda, I. Mochida, Adv. Catal. 42 (1998) 345.
[3] M. Houalla, N.K. Nag, A.V. Sapre, D.H. Broderick, B.C. Gates, AIChE J. 24 (1978) 1015.
[4] T. Fujikawa, K. Tsuji, H. Mizuguchi, H. Godo, K. Idei, K. Usui, Catal. Lett. 63 (1999) 27.
[5] L. Simon, J.G. van Ommen, A. Jentys, J.A. Lercher, J. Phys. Chem. B 104 (2000) 11644.
[6] L. Simon, J.G. van Ommen, A. Jentys, J.A. Lercher, J. Catal. 201 (2001) 60.
[7] L. Simon, J.G. van Ommen, A. Jentys, J.A. Lercher, J. Catal. 203 (2001) 434.
[8] J.L. Rousset, L. Stievano, F.J. Cadete Santos Aires, C. Geantet, A.J. Renouprez, M. Pellarin, J. Catal. 197 (2000) 335.
[9] J.L. Rousset, L. Stievano, F.J. Cadete Santos Aires, C. Geantet, A.J. Renouprez, M. Pellarin, J. Catal. 202 (2001) 163.
[10] R.M. Navarro, B. Pawelec, J.M. Trejo, R. Mariscal, J.L.G. Fierro, J. Catal. 189 (2001) 184.
[11] K. Thomas, C. Binet, T. Chevreau, D. Cornet, J.P. Gilson, J. Catal. 212 (2002) 63.
[12] S. Albertazzi, G. Busca, E. Finocchio, R. Glöckler, A. Vaccari, J. Catal. 223 (2004) 372.
[13] E. Rodríguez-Castellón, J. Mérida-Robles, L. Díaz, P. Maireles-Torres, D.J. Jones, J. Rozière, A. Jiménez-López, Appl. Catal. A 260 (2004) 9.
[14] R. Navarro, B. Pawelec, J.L.G. Fierro, P.T. Vasudevan, J.F. Cambra, P.L. Arias, Appl. Catal. A 137 (1996) 269.
[15] W.R.A.M. Robinson, J.A.R. van Veen, V.H.J. de Beer, R.A. van Santen, Fuel Process. Technol. 61 (1999) 103.
[16] H.R. Reinhoudt, R. Troost, S. van Schalkwijk, A.D. van Langeveld, S.T. Sie, J.A.R. van Veen, J.A. Moulijn, Fuel Process. Technol. 61 (1999) 117.
[17] T. Kabe, W. Qian, Y. Hirai, L. Li, A. Ishihara, J. Catal. 190 (2000) 191.
[18] V.L. Barrio, P.L. Arias, J.F. Cambra, M.B. Güemez, B. Pawelec, J.L.G. Fierro, Fuel 82 (2003) 501.
[19] W. Qian, K. Otani, L. Li, A. Ishihara, T. Kabe, J. Catal. 221 (2004) 294.
[20] M. Egorova, R. Prins, J. Catal. 221 (2004) 11.
[21] T. Matsui, M. Harada, K.K. Bando, M. Toba, Y. Yoshimura, Appl. Catal. A 290 (2005) 73.
[22] M. Egorova, R. Prins, J. Catal. 225 (2004) 417.
[23] P. Kukula, A. Dutly, R. Prins, in preparation.
[24] M. Egorova, R. Prins, J. Catal. 224 (2004) 278.
[25] T. Kabe, A. Ishihara, Q. Zhang, Appl. Catal. A 97 (1993) L1.
[26] D.H. Broderick, B.C. Gates, AIChE J. 27 (1981) 663.